Electrically Active Convection in Tropical Easterly Waves and Implications for Tropical Cyclogenesis in the Atlantic and East Pacific

KENNETH D. LEPPERT II

University of Alabama in Huntsville, Huntsville, Alabama

WALTER A. PETERSEN

NASA GSFC/Wallops Flight Facility Field Support Office, Wallops Island, Virginia

DANIEL J. CECIL*

University of Alabama in Huntsville, Huntsville, Alabama

(Manuscript received 15 June 2012, in final form 2 August 2012)

ABSTRACT

In this study, the authors investigated the characteristics of tropical easterly wave convection and the possible implications of convective structure on tropical cyclogenesis and intensification over the Atlantic Ocean and the east Pacific Ocean. Easterly waves were partitioned into northerly, southerly, trough, and ridge phases based on the 700-hPa meridional wind from the National Centers for Environmental Prediction–National Center for Atmospheric Research reanalysis dataset. Waves were subsequently divided according to whether they did or did not develop tropical cyclones (i.e., developing and nondeveloping, respectively), and developing waves were further subdivided according to development location. Finally, composites as a function of wave phase and category were created using data from the Tropical Rainfall Measuring Mission (TRMM) Microwave Imager, Precipitation Radar (PR), and Lightning Imaging Sensor as well as infrared (IR) brightness temperature data from the NASA global-merged IR brightness temperature dataset.

Results suggest that the convective characteristics that best distinguish developing from nondeveloping waves vary according to where developing waves spawn tropical cyclones. For waves that develop a cyclone in the Atlantic basin, coverage by IR brightness temperatures $\leq$240 and $\leq$210 K provide the best distinction between developing and nondeveloping waves. In contrast, several variables provide a significant distinction between nondeveloping waves and waves that develop cyclones over the east Pacific as these waves near their genesis location including IR threshold coverage, lightning flash rates, and low-level ($<$4.5 km) PR reflectivity. Results of this study may be used to help develop thresholds to better distinguish developing from nondeveloping waves and serve as another aid for tropical cyclogenesis forecasting.

1. Introduction

African easterly waves (AEWs) form in the tropical easterlies over east-central Africa (e.g., Burpee 1972; Norquist et al. 1977; Reed et al. 1977; Berry and Thorncroft 2005; Thorncroft et al. 2008) and often form the necessary precursor low-level disturbance for tropical cyclogenesis (Kurihara and Tuleya 1981). These waves are important for tropical cyclogenesis not only in the Atlantic Ocean (e.g., Landsea 1993), but also in the east Pacific Ocean (e.g., Avila 1991; Avila and Pasch 1992; Molinari and Vollaro 2000; note, however, that not all easterly waves found over the east Pacific originate over Africa; e.g., Serra et al. 2008, 2010).

One outstanding question is why some waves develop tropical cyclones while others do not. By definition, organized deep convection is necessary but not sufficient for the development of a tropical cyclone. Differences in the nature of convection between different waves may be one determinant for why some waves develop

* Current affiliation: NASA Marshall Space Flight Center, Huntsville, Alabama.

Corresponding author address: Kenneth Leppert II, NSSTC, 320 Sparkman Dr., Rm. 4074, Huntsville, AL 35805.
E-mail: leppert@nsstc.uah.edu

DOI: 10.1175/MWR-D-12-00174.1

while others do not. Hence, this study examines various observations/characteristics of convection associated with developing waves and nondeveloping waves (NDWs) to determine which characteristics of convection provide the best distinction between the two wave types and may be most important for tropical cyclogenesis.

Via thermodynamic and dynamic feedbacks between the smaller convective scale and larger synoptic scale, more intense and/or widespread convection associated with developing waves could help to produce conditions in the wave more favorable for development. For example, one possible effect of convection on the larger scale favorable for tropical cyclogenesis is an increase in mid- to low-level vorticity (e.g., Ritchie and Holland 1997; Hendricks et al. 2004; Reasor et al. 2005; Montgomery et al. 2006; Sippel et al. 2006; Houze et al. 2009). Another potential contribution of persistent, widespread convection to the genesis process is the moistening of mid- and upper levels via transport of moisture from the surface (e.g., Rotunno and Emanuel 1987; Nolan 2007; Dunkerton et al. 2009).

Because enhanced convection could potentially enhance the development of an easterly wave circulation and structure more favorable for tropical cyclogenesis, it is not surprising that previous studies have found developing waves to be associated with more intense and/or widespread convection compared to NDWs. For example, Hopsch et al. (2010) used IR brightness temperatures to determine that developing waves are, in fact, associated with more widespread/intense convection. Chronis et al. (2007) used lightning frequency to infer the intensity of convection and found that tropical cyclogenesis in the east Atlantic may be related to enhanced electrical activity (i.e., more intense convection) over that region. In this case, lightning represents a proxy for deep convective updrafts and robust mixed-phase microphysical processes, previously demonstrated to be a prerequisite for the development of strong in-cloud electric fields and associated lightning (e.g., Takahashi 1978; Rutledge et al. 1992; Williams et al. 1992; Zipser 1994; Saunders and Peck 1998; Deierling and Petersen 2008). In addition, Price et al. (2007) showed that enhanced lightning over East Africa may also be associated with cyclogenesis over the east Atlantic. Leary and Ritchie (2009) examined cloud clusters instead of waves in the east Pacific and found that developing cloud clusters were associated with significantly more lightning than nondeveloping clusters. Leppert and Petersen (2010, hereafter LP10) examined IR brightness temperatures as well as lightning associated with AEWs over several longitude bands stretching from East Africa (30°E) to the central Atlantic (50°W). They found that over each longitude band developing waves were associated with a greater coverage of more intense, electrically active convection compared to NDWs.

This study expands on previous studies by not only by examining lightning and/or IR brightness temperatures for clues about convection related to tropical cyclogenesis but also by examining microwave brightness temperatures from the Tropical Rainfall Measuring Mission (TRMM) Microwave Imager (TMI) and radar reflectivity data from the TRMM Precipitation Radar (PR). In particular, the purpose of this study is twofold: 1) determine which observations/characteristics of convection provide the best distinction between developing waves and NDWs and 2) determine whether the characteristics that provide the best distinction vary for waves that develop tropical cyclones over different regions. This paper composites all easterly wave observations over fixed regions (i.e., Eulerian framework), while a companion study (Leppert and Cecil 2012) examines composites in a wave-following, Lagrangian sense. The Eulerian methodology and the associated results from this paper could potentially be used to help distinguish developing waves from NDWs for forecasting applications. In contrast, the Lagrangian methodology used in Leppert and Cecil (2012) requires a priori information describing when and where a wave developed a tropical cyclone, limiting its direct application to the forecasting process. However, the Lagrangian framework can provide information on the evolution of waves in the days leading up to cyclogenesis (i.e., a greater understanding of the genesis process) that cannot be obtained from the Eulerian approach.

2. Data and methodology

Following the methodology of LP10, 700-hPa meridional wind data from the National Centers for Environmental Prediction–National Center for Atmospheric Research (NCEP–NCAR) reanalysis (Kalnay et al. 1996) [spatial resolution of 2.5° and a temporal resolution of 6 h (averaged to 1 day for this study)] were used to analyze easterly waves and separate them into phases (ridge, northerly, trough, and southerly phases). Specifically, the various wave phases were identified by first calculating a daily average meridional wind value between 5°–20°N and then calculating a meridional wind anomaly (relative to the mean at each longitude) for each day and longitude. Next, a 3–7-day bandpass filter was applied to the anomalies in order to isolate the period of the easterly waves. The filtered anomalies were subsequently normalized by the standard deviation valid at each longitude, and the ± 0.75 standard deviation threshold was used to identify the individual wave phases. In particular, normalized anomalies greater (less) than

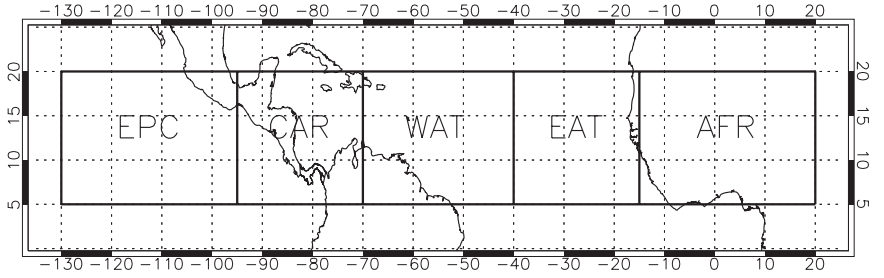

FIG. 1. Map showing the location of the full analysis domain (130°W–20°E) and smaller longitude bands utilized for this study. EPC represents the east Pacific band, CAR the Caribbean and Central America band, WAT the west Atlantic band, EAT the east Atlantic band, and AFR the Africa longitude band.

0.75 (−0.75) were classified as the southerly (northerly) phase. For a given day, values between northerly (southerly) and southerly (northerly) phases were identified as trough (ridge) phases. Finally, to classify many of those data points unable to be classified using meridional wind data alone, 700-hPa vorticity was calculated using reanalysis zonal and meridional wind components and processed exactly as the meridional wind data (i.e., meridional and daily averages of vorticity were calculated, anomalies were calculated and bandpass filtered, the resulting values were normalized by the standard deviation, and the ±0.75 threshold was used to identify wave phases).

The analysis domain over which the wave phases were identified for this study was larger than that used in LP10 and stretched from 130°W to 20°E and from 5° to 20°N, outlined in Fig. 1. To examine the evolution of convection and cold cloudiness associated with the waves as they propagated through our analysis domain, the full analysis domain was divided into five longitude bands, also shown in Fig. 1. These bands stretched from 130° to 95°W over the east Pacific (EPC), from 95° to 70°W over the western Caribbean and far eastern Pacific region (CAR; this band includes the Central American landmass as well as the northern part of South America), from 70° to 40°W over the west Atlantic (WAT), from 40° to 15°W over the east Atlantic (EAT; the eastern boundary of this band lies approximately along the West African coast), and from 15°W to 20°E over Africa (AFR). The waves were analyzed for the months of June–November for the 10-yr span of 2001–10. These are the months in which easterly waves are the most pronounced (e.g., Carlson 1969; Gu et al. 2004) and when tropical cyclones often develop in the Atlantic and east Pacific regions [National Hurricane Center (NHC) storm reports; National Hurricane Center 2011].

After the various wave phases were identified, the wave troughs were divided into developing (i.e., waves that developed tropical cyclones that attained at least tropical storm strength) and NDWs (i.e., waves that never developed a tropical cyclone; see Table 1 for acronyms and definitions of each wave category used in this study) via information provided by National Hurricane Center (2011). In addition, developing waves were divided based on the longitude band over which they developed a tropical depression. Once the trough phases were partitioned into various categories, any of the other three wave phases found within three data points (7.5°) east or west of each wave trough were considered to be part of that wave and used in the composites.

The Lightning Imaging Sensor (LIS) on board TRMM consists of an optical imager capable of recording brief radiance events associated with lightning (Christian et al. 1992; Boccippio et al. 2002) with an estimated detection efficiency of 70%–90% (Christian 1999; Boccippio et al. 2000, 2002; no correction for detection efficiency was utilized for the current study). In particular, we used the 0.5° LIS flash counts and view time data to compute the lightning flash density over 0.5° boxes and subsequently averaged these values over 2.5° grid boxes for each day.

The PR is a phased array radar system operating at 13.8 GHz (Kummerow et al. 1998; Kozu et al. 2001).

TABLE 1. Definitions and acronyms associated with various wave categories used in this study.

Wave category	Acronym	Definition
East Atlantic developing wave	EADW	Wave developed a tropical depression over the east Atlantic longitude band
West Atlantic–Caribbean developing wave	WACDW	Wave developed a tropical depression over the west Atlantic or Caribbean longitude band
East Pacific developing wave	EPDW	Wave developed a tropical depression over the east Pacific longitude band
Nondeveloping wave	NDW	Wave never developed a tropical cyclone of at least tropical storm strength

Specifically, attenuation-corrected radar reflectivity (Iguchi et al. 2000; Meneghini et al. 2000; Iguchi et al. 2009) and a convective/stratiform classification (Awaka et al. 1998, 2009) from the PR 2A25 V6.0 product were utilized for this study. The reflectivity values classified as convective were used to calculate mean convective reflectivity profiles for each 2.5° box with 1-km height resolution from 1–18 km above ground level. Only convective rays of data with a rain bottom below 2 km and not classified as warm rain were used in the construction of these mean profiles to isolate the type of convection presumably most relevant for tropical cyclogenesis.

The convective rain classification from 2A25 V6.0 was also used to tabulate the percentage convective coverage over each 2.5° box. Another coverage parameter was calculated using data from the 4-km National Aeronautics and Space Administration (NASA) global-merged IR brightness temperature dataset (Liu et al. 2009). Specifically, the fractional coverage by IR brightness temperatures $\leq$210 and $\leq$240 K over each 2.5° box was calculated to examine the coverage by cold cloudiness.

The TMI instrument is a nine-channel passive microwave radiometer (Kummerow et al. 1998). Four TMI channels were used in this study, including the 37.0- and 85.5-GHz horizontally and vertically polarized channels. The measured radiances in these channels are especially sensitive to scattering by ice (e.g., Spencer et al. 1989; Smith et al. 1992; Cecil and Zipser 1999; Toracinta et al. 2002). Significant scattering and an accompanying reduction in the measured brightness temperatures at 85.5 GHz can be accomplished by relatively small ice particles ($\sim 10^{-4}$ m in diameter), but significant reductions in brightness temperatures at 37.0 GHz require the presence of larger (millimeter sized) particles (Toracinta et al. 2002). Therefore, a significant reduction in 37.0-GHz brightness temperatures likely indicates a stronger updraft and more intense convection required for the formation and maintenance of large ice particles in the upper portions of clouds. The 85.5-GHz channel has also been used in several earlier studies to characterize the intensity and spatial extent of convection (e.g., Mohr and Zipser 1996; Cecil and Zipser 1999; Mohr et al. 1999).

At 37.0 and 85.5 GHz, variations in surface emissivity and temperature can lead to large variations in brightness temperature unrelated to the overlying atmosphere. To remove these variations, we combined temperatures measured from both 85.5-GHz channels into 85.5-GHz polarization-corrected temperatures (PCT_{85}) as defined by Spencer et al. (1989). Similarly, the two 37.0-GHz channels were combined to form PCT_{37} as defined by Toracinta et al. (2002) and Cecil et al. (2002). Cecil and Zipser (2002) found that vigorous convection was generally present when PCT_{85} were below ~200 K and PCT_{37} were below ~263 K. Hence, only TMI pixels with $PCT_{85} \leq 200$ K and $PCT_{37} \leq 260$ K were used to calculate an average PCT_{85} and PCT_{37} over each 2.5° box.

Lightning flash rates, mean convective reflectivity profiles, mean PCTs, percentage convective coverage values, and IR fractional coverage values were subsequently composited as a function of wave phase for the different wave types over the various longitude bands (Fig. 1). Note that some developing wave composites were not created over every longitude band because after initial tropical cyclone development, developing waves were no longer tracked. For example, composites were created for waves that spawn tropical cyclones over the east Atlantic [i.e., east Atlantic developing waves (EADWs)] over only the Africa and east Atlantic longitude bands. EADWs were tracked up until they developed cyclones over the east Atlantic but not farther west.

The parameters we analyze here basically relate to either the areal coverage of convection (percentage convective coverage, coverage below IR brightness temperature thresholds) or the vigor of convection that does occur (lightning flash rate, mean PCTs for pixels below certain thresholds, and mean convective reflectivity). The IR thresholds (210 and 240 K) go beyond characterizing the convective area as cold anvils expand. Flash rate is somewhat related to both the coverage and intensity of convection, but one or more elements of intense convection can dominate this parameter much more than a large number of weak convective cells would. The PCT thresholds used here restrict the analysis to only pixels related to strong, deep convection. Hence, our mean PCT values are indicative of how strong that convection is when it does occur. [Note that taking the mean PCT without using thresholds (not shown) would be more related to the rain area and would be quite different than the mean PCTs with thresholds.] Similarly, our mean reflectivity values consider only the pixels that are already classified as convective, so they relate to the strength of that convection.

To test whether values from developing waves and NDWs are significantly different, the analysis of variance statistical technique was used. This technique provides an estimate of the error variance associated with some group of data and an estimate of the systematic variance between groups of data. If the systematic variance is greater than the error variance, then the *f* statistic is used to test whether the systematic effect is significantly greater than the random error effect. A significantly greater systematic effect suggests a high probability that differences between groups of data are, indeed, real and not just due to chance. Note for this study that a difference

TABLE 2. The number of distinct easterly waves and data points used for the trough composites of NDWs, EADWs, WACDWs, and EPDWs. The numbers of distinct waves are valid over the full analysis domain (ALL) while the trough points are valid over individual longitude bands (bands defined as in Fig. 1). The italics indicate wave categories that are valid for July–August only. The number of individual NDWs is an estimate and includes an estimate of uncertainty because of the difficulty in counting these waves (see text). Finally, the missing values are for those composites that were unavailable.

	Sample sizes					
	Distinct AEWs	Trough points				
	ALL	EPC	CAR	WAT	EAT	AFR
NDW	330 ± 40	2582	1695	1978	1737	2505
EADW	28	—	—	—	138	313
WACDW	37	—	102	290	317	436
EPDW	68	267	358	361	287	392
NDW	100 ± 15	612	449	467	454	573

is considered to be significant if the *f* statistic indicates significance at or above the 99% level. However, we do discuss some differences that do not satisfy the 99% level, if they contribute to a consistent understanding along with the other results. Additional information on the analysis of variance technique can be found in Panofsky and Brier (1958).

3. Results

a. *Comparison between east Atlantic developing waves and NDWs*

Table 2 shows the number of distinct easterly waves and the number of individual data points included in the trough phase composites of various wave categories, including EADWs and NDWs. Note that as a result of wave merger/splitting as well as the ambiguities associated with counting weak NDWs that alternately can be tracked for a short time over the analysis domain and then become too weak to be tracked, the number of distinct NDWs in Table 2 is only an estimate.

The composite coverage by IR brightness temperature thresholds are provided in Table 3 over various longitude bands for various wave categories, including for EADWs and NDWs. Over Africa, the coverage by temperatures ≤210 and ≤240 K is significantly greater in all EADW phases (except for the 210-K threshold in the trough phase) compared to the corresponding NDW values. Over the east Atlantic, significantly greater EADW values are confined to only the trough and northerly phases. Similarly, the composite percentage convective coverage values for EADWs and NDWs in Table 4 indicate that coverage is greater for EADWs over both Africa and the east Atlantic in each wave phase, except the ridge phase over the east Atlantic. The differences between EADWs and NDWs in the northerly phase over both Africa and the east Atlantic are significant, and the difference between trough phase values over the east Atlantic is also relatively large (while not significant at the 99% level, it is significant at the 95% level). Thus, as EADWs approach their genesis region over the east Atlantic, the maximum convective and cold cloudiness coverage occurs ahead of and within the wave trough where it may interact with the larger-scale wave helping to amplify the wave, perhaps making it more favorable for cyclogenesis (LP10).

TABLE 3. The fractional coverage by IR brightness temperatures ≤240 and ≤210 K for EADW, WACDW, and NDW phases valid over various longitude bands. The bold (italic) numbers indicate values that are significantly greater (less) than the corresponding NDW values valid at the 99% level.

	240 K				210 K			
	Ridge	Northerly	Trough	Southerly	Ridge	Northerly	Trough	Southerly
Africa								
EADW	**0.097**	**0.111**	**0.088**	**0.082**	**0.017**	**0.021**	0.015	**0.014**
WACDW	0.068	**0.085**	**0.083**	**0.079**	0.013	**0.017**	**0.015**	**0.013**
NDW	0.061	0.073	0.071	0.065	0.010	0.014	0.013	0.010
East Atlantic								
EADW	0.064	**0.094**	**0.094**	0.085	0.006	**0.009**	**0.010**	0.009
WACDW	0.046	0.064	**0.086**	*0.069*	0.004	0.004	**0.008**	0.005
NDW	0.072	0.059	0.075	0.088	0.005	0.004	0.006	0.007
West Atlantic								
WACDW	0.077	**0.067**	**0.103**	**0.110**	0.007	**0.008**	**0.011**	**0.015**
NDW	0.062	0.045	0.056	0.068	0.005	0.004	0.005	0.006
Caribbean								
WACDW	0.148	**0.162**	**0.169**	**0.163**	0.025	**0.029**	**0.032**	0.029
NDW	0.116	0.119	0.130	0.131	0.017	0.019	0.022	0.022

TABLE 4. Percentage convective coverage as a function of wave phase for EADWs, WACDWs, and NDWs valid over various longitude bands. The bold numbers indicate values that are significantly greater than the corresponding NDW values valid at the 99% level.

	Ridge	Northerly	Trough	Southerly
Africa				
EADW	1.11	**1.16**	0.96	0.91
WACDW	0.74	0.91	0.86	0.89
NDW	0.78	0.76	0.80	0.78
East Atlantic				
EADW	0.98	**1.48**	1.41	1.18
WACDW	1.18	1.07	1.24	1.10
NDW	1.02	1.07	1.16	1.11
West Atlantic				
WACDW	1.44	1.42	**1.70**	1.59
NDW	1.25	1.33	1.43	1.46
Caribbean				
WACDW	1.77	2.03	1.76	1.81
NDW	1.70	1.66	1.78	1.73

TABLE 5. As in Table 4, but for lightning flash rates [flashes per day per $(0.5°)^2$].

	Ridge	Northerly	Trough	Southerly
Africa				
EADW	223.2	179.6	266.1	214.2
WACDW	**587.0**	194.6	345.5	287.5
NDW	163.9	154.4	209.6	240.8
East Atlantic				
EADW	2.3	3.1	**64.7**	13.7
WACDW	0.7	2.7	9.4	12.6
NDW	2.5	9.8	4.5	19.0
West Atlantic				
WACDW	19.7	31.8	31.1	20.0
NDW	22.6	32.0	43.3	24.1
Caribbean				
WACDW	68.4	**609.9**	516.5	250.3
NDW	249.3	212.9	292.2	195.6

The differences in composite lightning flash rates (Table 5) between EADWs and NDWs over Africa are not significant, but all EADW phases, except the southerly phase, are associated with slightly higher flash rates than the corresponding NDW phases. The EADW southerly phase value is slightly smaller than that of NDWs over Africa. Consistent with several previous studies that show a decrease in lightning over the ocean compared to land (e.g., Christian et al. 2003), lightning decreases substantially over the east Atlantic compared to Africa. Except in the trough phase, all EADW flash rates over the east Atlantic are slightly less than those of NDWs. The EADW flash rate in the trough phase over the east Atlantic is significantly greater than the corresponding NDW value. Thus, other than the values in the trough phase over the east Atlantic, the lightning data suggest that convective intensity is comparable between the two wave types over both Africa and the east Atlantic.

Table 6 shows PCT_{37} and PCT_{85} values as a function of wave phase for various wave types and regions. Differences between EADWs and NDWs over both Africa and the east Atlantic are quite small and are not significant in any phase. Hence, an analysis of mean cold PCT values suggests little difference in the intensity of convection between EADWs and NDWs.

The difference between mean convective reflectivity values of EADWs and NDWs (EADW minus NDW values) as a function of wave phase valid over the east Atlantic is shown in Fig. 2. Note that differences are

TABLE 6. Mean polarization corrected temperatures at 37.0 and 85.5 GHz using 37.0-GHz values ≤260 K and 85.5-GHz values ≤200 K (i.e., values associated with deep convection) for EADW, WACDW, and NDW phases valid over various longitude bands. No EADW or WACDW values are significantly different from those of NDWs valid at the 99% level.

	37.0				85.5			
	Ridge	Northerly	Trough	Southerly	Ridge	Northerly	Trough	Southerly
Africa								
EADW	250.3	251.0	251.2	251.9	174.9	175.8	177.0	177.1
WACDW	251.5	252.2	251.6	251.6	175.1	176.0	176.3	176.1
NDW	251.4	251.7	251.7	251.7	176.4	176.4	177.0	177.7
East Atlantic								
EADW	257.4	256.4	256.5	256.1	185.9	184.0	184.3	183.0
WACDW	254.4	256.8	256.6	256.4	185.9	184.3	185.0	185.3
NDW	257.0	257.0	256.7	256.2	186.3	185.3	185.6	185.3
West Atlantic								
WACDW	255.8	254.5	255.2	255.5	183.7	181.5	183.5	182.2
NDW	255.3	254.7	255.3	255.6	183.0	182.0	183.1	183.4
Caribbean								
WACDW	255.5	252.6	253.2	253.3	181.0	177.5	177.4	178.4
NDW	253.7	253.5	253.3	253.2	178.0	178.6	178.6	178.5

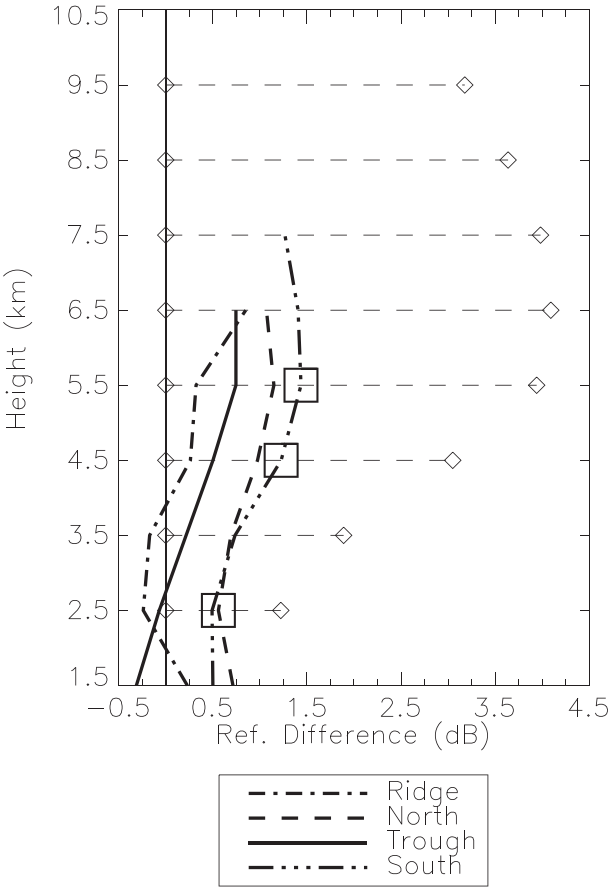

FIG. 2. The PR convective reflectivity (only values classified as convective are used) differences between EADWs and NDWs (i.e., EADW minus NDW values) as a function of height and wave phase valid over the east Atlantic. The dashed horizontal lines depict the value of the standard deviation at each height, and the squares indicate EADW values that are significantly greater than the corresponding values of NDWs valid at the 99% level.

calculated and shown in Fig. 2 and all subsequent figures only where the mean reflectivity values for both developing waves and NDWs are ≥18 dBZ (the approximate minimum detectable signal of the PR; Yang et al. 2006). Differences are generally positive in Fig. 2, indicating greater reflectivity values for EADWs. These larger reflectivity values would presumably be associated with stronger updrafts and more vigorous convection in order to support such reflectivity values. However, only the value at 2.5 km in the northerly phase and 4.5–5.5 km in the southerly phase are significantly greater for EADWs (indicated by squares in Fig. 2). Thus, considering how many levels and phases fail the significance tests, we cannot infer much from the few levels that do show significance. In addition, the differences between EADW and NDW reflectivity profiles over Africa (not shown) are also small and not statistically significant.

In summary, EADWs appear to be associated with a greater *coverage* by convection and cold cloudiness over both Africa and the east Atlantic compared to NDWs. There is only slight indication of more intense convection associated with EADWs. These results are generally consistent with the results of LP10 where developing waves were found to be associated with a greater coverage by cold cloud tops and more lightning compared to NDWs. The coverage by IR brightness temperatures ≤240 and/or ≤210 K provide the greatest number of statistically significant differences between EADWs and NDWs over both Africa and the east Atlantic, thus, providing the best discrimination between EADWs and NDWs.

Some waves included in the NDW composite are associated with relatively little cold cloudiness and convection and, from an operational forecasting perspective, would clearly be distinguished from developing waves. Hence, a comparison between these NDWs and developing waves is not particularly instructive. To make a comparison between developing waves and NDWs associated with a similar probability of development, the archived Graphical Tropical Weather Outlooks produced by the NHC were examined in order to identify easterly waves that were assigned a moderate (30%–50%) chance of genesis within 48 h. Composites were created for NDWs and all developing waves in 2009 and 2010 (the archived outlooks were only available for the last two years of the study) at the times and locations when these waves were assigned a 30%–50% chance of genesis by the NHC. Forty-two (117) distinct easterly waves (individual trough data points) were included in these developing wave composites. Note that 40 of these 42 waves actually developed within 48 h. Nine (42) distinct waves (trough points) were included in the NDW composites. Table 7 shows the statistics for these 30%–50% chance-of-genesis developing and NDW composites valid over the full analysis domain (to maximize the sample size). Coverage by IR brightness temperatures ≤240 K, convective coverage, and flash rates are greater in nearly all developing wave phases compared to the corresponding NDW phases with the greatest differences generally found in the trough and northerly phases. In addition, PCT_{37} values are smaller in all developing wave phases, except the southerly phase. Therefore, when developing and NDWs were associated with an enhanced probability of cyclogenesis according to the NHC, developing waves appear to be associated with more widespread and intense convection, in general, in agreement with the results of the comparison between all NDWs and EADWs. Note that none of the variables show statistically significant differences between developing waves and NDWs associated with a moderate

TABLE 7. The fractional coverage by IR brightness temperatures ≤240 and ≤210 K, mean polarization corrected temperatures (K) at 37.0 and 85.5 GHz using the same thresholds as in Table 6, convective coverage (%), and lightning flash rates [flashes per day per $(0.5°)^2$] for developing and nondeveloping waves (30%–50% developing and 30%–50% nondeveloping, respectively) that were assigned a 30%–50% probability of development within the next 48 h by the National Hurricane Center. Note that none of the 30%–50% developing values are significantly different from the corresponding 30%–50% nondeveloping values valid at the 99% level.

		Ridge	Northerly	Trough	Southerly
IR brightness temperature thresholds					
30%–50% developing	240 K	0.108	0.115	0.154	0.172
	210 K	0.011	0.014	0.021	0.024
30%–50% nondeveloping	240 K	0.104	0.079	0.133	0.125
	210 K	0.015	0.009	0.021	0.021
Polarization corrected temperatures					
30%–50% developing	37.0	254.7	254.7	255.0	255.4
	85.5	185.4	182.1	182.2	183.0
30%–50% nondeveloping	37.0	255.7	256.7	256.1	255.0
	85.5	180.1	183.1	183.6	180.6
Convective coverage					
30%–50% developing		1.56	1.48	1.93	1.93
30%–50% nondeveloping		1.62	1.20	1.38	1.69
LIS flash rates					
30%–50% developing		58.1	30.2	38.6	65.1
30%–50% nondeveloping		103.3	4.0	6.5	58.4

probability of genesis, possibly due to relatively small sample sizes.

The climatological peak of tropical cyclone occurrence in the Atlantic occurs around August–September (e.g., Landsea 1993). Hence, we wanted to examine possible intraseasonal impacts on our results by examining a comparison between EADWs and NDWs valid only for August–September. In general, this comparison (not shown) revealed patterns similar to those found for the comparison valid for June–November, especially over the east Atlantic (i.e., greater coverage and/or intensity of convection for EADWs). However, the magnitude of differences between the two wave categories valid for the shortened time period were somewhat smaller and less often statistically significant than observed for the comparison valid for the full time period. Restricting the NDW composite to those waves that occur in August–September may lead to a composite of waves that presumably propagate through an environment climatologically more favorable for cyclogenesis (e.g., moister environment) and for more widespread/intense convection compared to the full June–November sample.

b. Comparison between west Atlantic–Caribbean developing waves and NDWs

To increase the sample size (Table 2), waves that developed a tropical cyclone over either the west Atlantic or Caribbean were combined into a single category [i.e., west Atlantic–Caribbean developing waves (WACDWs)]. The coverage by IR brightness temperatures ≤240 and ≤210 K shown in Table 3 indicate that WACDWs are associated with significantly greater coverage by cold cloud tops compared to NDWs in all phases except the ridge over Africa, the west Atlantic, and the Caribbean (the WACDW southerly phase 210-K threshold value over the Caribbean is greater than the corresponding NDW value, but not significantly so). WACDW ridge values over these regions are also greater than those of NDWs, but not with 99% level significance. Over the east Atlantic, only the coverage by cold cloud tops in the trough phase is significantly greater for WACDWs. The coverage by cold cloudiness in other WACDW phases over the east Atlantic is generally less than the corresponding NDW values (the 240-K threshold in the southerly phase is actually significantly less). Thus, a persistent large coverage by cold cloudiness in the trough phase may be important for the genesis of tropical cyclones from WACDWs, while coverage by cold cloud tops in the ridge phase is relatively unimportant for genesis.

The percentage convective coverage values shown for WACDWs and NDWs in Table 4 indicate few significant differences between the two wave categories over any longitude band. In fact, only the WACDW trough over the west Atlantic is associated with significantly more convective coverage than the NDW trough. The coverage in the WACDW northerly phase over the Caribbean is also much greater than the corresponding NDW value, but the difference is only significant at the 95% level. Otherwise, convective coverage is generally comparable to or slightly greater for WACDWs compared to NDWs without significant differences.

The WACDW lightning flash rates (Table 5) are generally comparable to those of NDWs over all longitude bands, with few significant differences. In addition, the mean PCTs from deep convection in WACDWs (Table 6) suggest no significant differences between WACDW and NDW values with some values slightly greater for WACDWs and others slightly greater for NDWs. Hence, the intensity of convection associated with WACDWs as indicated by lightning and low PCTs does not appear to be all that different from that of NDWs.

The differences between mean vertical profiles of convective reflectivity for WACDWs and NDWs as a function of wave phase over various longitude bands are shown in Fig. 3. Over Africa, NDWs are generally associated with greater reflectivity values in all phases, except the northerly phase. In contrast, as WACDWs approach their genesis region over the Caribbean, reflectivity values are greater for these waves relative to NDWs at all heights in all phases, except the ridge. However, very few of the differences between WACDWs and NDWs over any longitude band are statistically significant. Only values at 3.5–4.5 km in the northerly phase over the Caribbean and 3.5–5.5 km in the trough over the west Atlantic are significantly greater for WACDWs. Hence, as WACDWs move from their origin over Africa to where they develop tropical cyclones over the west Atlantic and Caribbean, convective reflectivity values associated with these waves generally increase slightly relative to NDWs.

Similar to EADWs, the coverage by cold cloudiness (i.e., using IR thresholds) provides the greatest number of statistically significant differences between WACDWs and NDWs and appears to be the best discriminator between these two wave types, especially within the trough phase. While convective coverage, lightning flash rates, mean cold PCTs, and convective reflectivity provide few statistically significant differences between WACDWs and NDWs, these variables appear to indicate that WACDWs may be associated with slightly greater coverage and intensity of convection as these waves approach their genesis region. This enhancement of convection associated with WACDWs may help to moisten the larger-scale waves at the mid/upper levels (e.g., Dunkerton et al. 2009) and/or increase larger-scale mid- to low-level vorticity (e.g., Montgomery et al. 2006; Nolan 2007; Raymond et al. 2011), helping to create an environment more favorable for tropical cyclogenesis.

A comparison was also made between WACDWs and NDWs valid only for those months when WACDWs are most active (i.e., August–October) as indicated by the annual distribution of WACDW data points (not shown). Similar to EADWs, the restricted WACDW comparison generally did not change the results obtained from the full June–November comparison.

c. *Comparison between east Pacific developing waves and NDWs*

While east Pacific developing waves (EPDWs; i.e., waves which develop tropical cyclones over the east Pacific) are near their origin over Africa, they are obviously a long distance from where they develop tropical cyclones, and there are several complicating factors [e.g., the topography of Central America (Zehnder 1991; Mozer and Zehnder 1996; Farfan and Zehnder 1997; Zehnder et al. 1999) and barotropic instability over the Caribbean and east Pacific (Molinari et al. 1997)] that could influence an EPDW between Africa and the east Pacific. Hence, convection over Africa would not be expected to exert much of an influence on later tropical cyclogenesis over the east Pacific. Nevertheless, EPDW coverage by cold cloudiness valid for June–November (not shown) is significantly *greater* than that of NDWs in all wave phases over Africa. However, the June–November NDW composite over Africa includes all waves, including those waves that were too weak to track all the way across the Atlantic and waves with relatively little convection. A comparison between EPDW and NDW composites valid for only July and August (two of the most active months for tropical cyclogenesis in the east Pacific), which restricts the NDW composite to those waves that presumably move through an environment climatologically more favorable for convection and for cyclogenesis, shows a much different pattern than that observed for June–November. For example, the coverage by IR brightness temperatures below certain thresholds over Africa valid for July–August only (Table 8) shows *smaller* EPDW coverage in all phases (240-K threshold differences are significant in every phase, except the ridge phase, while 210-K differences are significant in the trough and northerly phases) compared to the corresponding NDW values. Thus, the focus of this subsection will be on a comparison between EPDWs and NDWs valid for July–August because this restricted comparison appears to provide more meaningful results than those obtained from the June–November comparison.

As EPDWs move over the east and west Atlantic, the coverage by cold cloudiness (Table 8) becomes comparable to that of NDWs with some values greater for EPDWs and other values greater for NDWs with no significant differences. Over the Caribbean and east Pacific, all IR threshold coverage values are greater for EPDWs. Values are significantly greater in the EPDW southerly phase over the Caribbean and all phases over

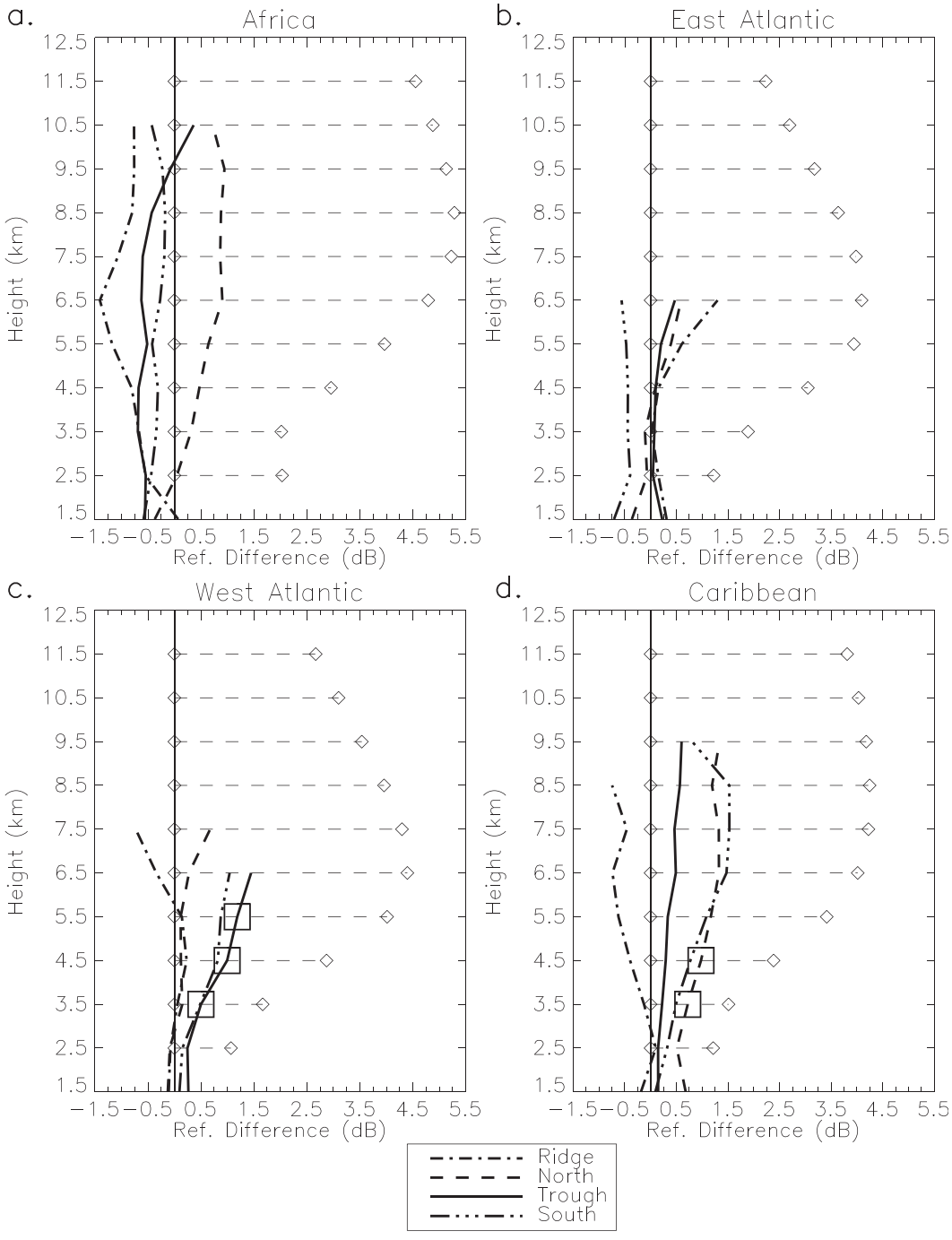

FIG. 3. The PR convective reflectivity (only values classified as convective are used) differences between WACDWs and NDWs (i.e., WACDW minus NDW values) as a function of height and wave phase valid over (a) Africa, (b) the east Atlantic, (c) the west Atlantic, and (d) the Caribbean. The dashed horizontal lines depict the value of half the standard deviation at each height, and the squares indicate WACDW values that are significantly greater than the corresponding NDW values valid at the 99% level.

the east Pacific (except for the 210-K value in the ridge). Convective coverage (not shown) is generally greater for NDWs over Africa, the east Atlantic, and west Atlantic, but differences between these waves and EPDWs are generally not significant. In contrast, convective coverage is often greater for EPDWs over the Caribbean and east Pacific with significantly greater values in the southerly phase over the Caribbean and northerly

TABLE 8. The fractional coverage by IR brightness temperatures ≤240 and ≤210 K for EPDW and NDW phases valid over various longitude bands using only data valid for July and August. The bold and italic values are as in Table 3.

	240 K				210 K			
	Ridge	Northerly	Trough	Southerly	Ridge	Northerly	Trough	Southerly
Africa								
EPDW	0.083	*0.100*	*0.093*	*0.068*	0.014	*0.017*	*0.016*	0.011
NDW	0.089	0.116	0.105	0.081	0.017	0.023	0.019	0.013
East Atlantic								
EPDW	0.054	0.048	0.057	0.049	0.004	0.003	0.004	0.002
NDW	0.048	0.052	0.064	0.053	0.003	0.003	0.005	0.004
West Atlantic								
EPDW	0.051	0.041	0.054	0.058	0.004	0.003	0.004	0.005
NDW	0.037	0.042	0.047	0.050	0.003	0.003	0.004	0.004
Caribbean								
EPDW	0.141	0.151	0.156	**0.166**	0.022	0.026	0.027	**0.029**
NDW	0.124	0.146	0.149	0.136	0.020	0.026	0.027	0.023
East Pacific								
EPDW	**0.099**	**0.130**	**0.154**	**0.180**	0.010	**0.016**	**0.022**	**0.024**
NDW	0.073	0.084	0.116	0.122	0.006	0.008	0.013	0.014

and southerly phases over the east Pacific. Thus, relative to NDWs, convective and cold cloudiness coverage is smaller for EPDWs over Africa and generally increases as EPDWs move across the Atlantic and approach their genesis region as would be expected.

Composite lightning flash rates for EPDWs and NDWs (Table 9) indicate that flash rates are generally greater for EPDWs over Africa compared to the corresponding NDW values, but differences are not significant. Over the east Atlantic, west Atlantic, and Caribbean, flash rates are comparable between EPDWs and NDWs with some values greater for EPDWs and others greater for NDWs. When EPDWs are over the east Pacific where they develop tropical cyclones, flash rates in all phases of these waves are greater (significantly greater in the northerly phase) than the corresponding NDW values.

A comparison between EPDW and NDW cold PCTs (not shown) indicates, similar to other developing waves, little difference between the two wave types. However, over the east Pacific, EPDW trough and southerly phase PCT_{85} values are significantly less than the corresponding NDW values, suggesting more intense convection for these waves near their genesis region. Overall, though, differences between developing waves (EADWs, WACDWs, and EPDWs) and NDWs in terms of mean cold PCTs are quite small over all longitude bands, suggesting that this way of comparing PCTs (taking the mean of pixels below a threshold for deep convection) may not be the best use of passive microwave information.

Over all longitude bands east of the east Pacific band, differences between EPDWs and NDWs in terms of mean convective reflectivity profiles (not shown) are generally small with few statistically significant differences. Differences in convective reflectivity profiles between EPDWs and NDWs over the east Pacific (Fig. 4) indicate generally greater values for EPDWs in all phases at all levels. EPDW values are significantly greater between 2.5 and 5.5 km in the northerly phase, at 2.5 km in the trough, and at 3.5 km in the southerly phase. Thus, when EPDWs are near their origin over Africa, differences between these waves and NDWs in terms of convective reflectivity are small. Differences remain small until EPDWs move over their genesis region of the east Pacific, where low- to midlevel reflectivity values become significantly greater for these waves in all phases other than the ridge.

TABLE 9. Lightning flash rates [flashes per day per $(0.5°)^2$] for EPDW and NDW phases valid over various longitude bands using only data valid for July and August. The bold numbers indicate values that are significantly greater than the corresponding NDW values valid at the 99% level.

	Ridge	Northerly	Trough	Southerly
Africa				
EPDW	216.4	221.1	235.9	366.7
NDW	174.5	170.1	278.1	233.5
East Atlantic				
EPDW	2.2	1.5	4.0	49.4
NDW	1.1	0.4	2.0	48.1
West Atlantic				
EPDW	10.8	19.8	57.9	41.0
NDW	9.3	38.6	94.0	20.4
Caribbean				
EPDW	193.4	312.5	231.8	417.2
NDW	584.9	445.1	353.0	251.6
East Pacific				
EPDW	43.8	**105.2**	66.1	104.4
NDW	62.2	32.3	41.0	61.7

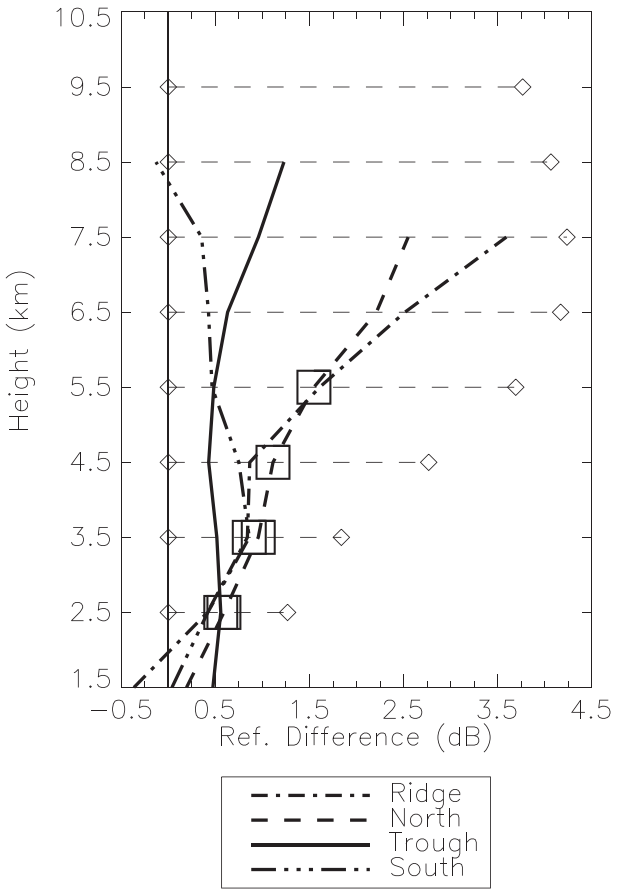

FIG. 4. The PR convective reflectivity (only values classified as convective are used) differences between EPDWs and NDWs (i.e., EPDW minus NDW values) as a function of height and wave phase valid over the east Pacific valid for July–August only. The dashed horizontal lines depict the value of half the standard deviation at each height, and the squares indicate EPDW values that are significantly greater than the corresponding NDW values valid at the 99% level.

In summary, EPDW convective coverage and/or intensity appear to be relatively low compared to NDWs near their origin over Africa. As EPDWs move across the Atlantic, Caribbean, and into the east Pacific region, convective coverage and/or intensity gradually become significantly greater than that of NDWs. The pronounced increase in convection over the Caribbean and east Pacific may be related to barotropic instability found over these regions (Molinari et al. 1997). It is possible that this instability over the Caribbean and east Pacific could help amplify easterly waves, perhaps helping to spawn more convection within the waves over these regions. In addition, the Caribbean region may be associated with an enhancement of convection due to the large landmasses in that region (cf. Fig. 1). Note that both EPDWs and NDWs are subject to the effects of land and its associated diurnal cycle of convection over the Caribbean region. Thus, any differences observed between these two wave types in terms of characteristics of convection should not be due to land–ocean differences.

In contrast to EADWs and WACDWs where the coverage by IR thresholds was clearly the one variable that could provide the best discrimination between these waves and NDWs, several variables could potentially be used to separate EPDWs from NDWs over the east Pacific, including IR thresholds, lightning flash rates, and low-level PR convective reflectivity values. Thus, indicators for both the intensity and coverage of convection over the east Pacific may be important for tropical cyclogenesis and distinguishing developing waves from NDWs over this region.

Based on National Hurricane Center (2011), some waves spawned a tropical cyclone in both the Atlantic and east Pacific basins. To determine if there were any differences in terms of convective characteristics between these waves that spawned multiple cyclones and those that spawned only one storm, composites were created for waves that developed multiple cyclones. However, few significant differences were found between multiple and single cyclone waves. Waves that develop multiple cyclones may lend themselves better to case study analysis, which is left for future work.

Again using information from the National Hurricane Center (2011), developing waves were also separated according to whether the subsequent tropical cyclone achieved hurricane strength or only tropical storm strength. Composites were also created for both of these wave categories. Except for some differences between hurricane and tropical storm waves over the west Atlantic, the convective characteristics of hurricane and tropical storm waves are generally not significantly different. These results are not surprising because many other factors (e.g., SSTs, wind shear, etc.) help control the final strength of a tropical cyclone. In addition, because we are not controlling for large-scale conditions, the relative enhancement of convection in hurricane waves over the west Atlantic could be a result of large-scale conditions favorable for both convection and intensification to hurricane strength. In this case, the enhanced convection in the precursor wave is not a factor responsible for intensification to hurricane strength.

4. Summary and conclusions

This study examines the characteristics of convection and cold cloudiness associated with tropical easterly waves using data from the Tropical Rainfall Measuring Mission (TRMM) Lightning Imaging Sensor, Precipitation Radar (PR), and Microwave Imager as well as IR brightness temperatures from the NASA global-merged

TABLE 10. A summary of the convective parameters that provide the greatest distinction between NDWs and EADWs, WACDWs, and EPDWs over various regions (EAT = east Atlantic, WAT = west Atlantic, CAR = Caribbean, and EPC = east Pacific) in various phases. Suggested thresholds to initially be tested to determine the utility of these parameters for tropical cyclogenesis forecasting are also provided. Note that the 240- and 210-K IR coverage thresholds are nondimensional, while the flash rate threshold has units of flashes per day per $(0.5°)^2$.

Wave type	Location	Phase	Parameter	Threshold
EADW	EAT	Northerly/ trough	240-K IR coverage	0.090
EADW	EAT	Northerly/ trough	210-K IR coverage	0.009
WACDW	WAT	Southerly	240-K IR coverage	0.085
WACDW	WAT	Southerly	210-K IR coverage	0.009
WACDW	CAR	Trough	240-K IR coverage	0.155
WACDW	CAR	Trough	210-K IR coverage	0.029
EPDW	CAR	Southerly	240-K IR coverage	0.150
EPDW	EPC	Trough/southerly	240-K IR coverage	0.140
EPDW	EPC	Northerly	Flash rate	60.0

dataset. In particular, the purpose of the study was to determine which characteristics or observations of convection provide the best distinction between developing waves and nondeveloping waves (NDWs) and over which regions. Another goal of the study was to determine whether the convective characteristics that provide the best distinction between the two wave types vary for waves that develop tropical cyclones over different regions.

Results suggest that the variables that provide the best distinction between developing waves and NDWs do vary between the Atlantic and east Pacific, and these variables are summarized in Table 10 for various developing wave categories and regions. In particular, the coverage by IR brightness temperatures $\leq$240 and $\leq$210 K appear to provide the largest distinction between east Atlantic developing waves (EADWs; waves that developed a tropical cyclone over the east Atlantic) and NDWs in all wave phases over Africa and in the trough and northerly phases over the east Atlantic. The coverage by IR thresholds also provides the best distinction between west Atlantic–Caribbean developing waves (WACDWs; waves that spawned a cyclone over either the west Atlantic or Caribbean) and NDWs. In particular, the coverage by cold cloudiness was found to be significantly greater for WACDWs in all phases, except the ridge, over all longitude bands but the east Atlantic (values are only significantly greater for WACDWs in the trough over the east Atlantic). Thus, results for WACDWs indicate that a persistent large coverage by cold cloudiness in the trough phase may be important for cyclogenesis from these waves. The indicators of convective intensity (i.e., lightning flash rates, polarization corrected temperatures, and convective reflectivity) generally suggest no significant differences between Atlantic developing waves and NDWs. This may be a result of similar large-scale environmental conditions (e.g., SSTs, trade wind inversion height, etc.) experienced by developing waves and NDWs over the Atlantic. The fact that indices of the coverage by convection/cold cloudiness provide a better discrimination between developing waves and NDWs over the Atlantic suggests that the coverage by convection is more important than the intensity of convection for tropical cyclogenesis over the Atlantic.

In contrast to waves that developed a tropical cyclone over the Atlantic basin, waves which spawned a tropical cyclone over the east Pacific [east Pacific developing waves (EPDWs)] are associated with statistically significantly greater IR threshold coverage, convective coverage, lightning flash rates, and low-level PR convective reflectivity in various wave phases (no clear preference for enhanced convection in any one wave phase over another) when compared to NDWs over the east Pacific. In contrast to what was found for EADWs and WACDWs, restricting the comparison between EPDWs and NDWs to only the most active months for east Pacific cyclogenesis led to quite different results from the corresponding comparison valid for June–November, especially over Africa. This suggests that care must be taken in selecting a temporal domain for a comparison between EPDWs and NDWs and/or selecting a sample of NDWs.

Future work could involve developing thresholds based on the most relevant convective parameters to help provide an indication of enhanced probability (or lack thereof) of tropical cyclogenesis. For example, Table 10 lists an initial threshold that could be tested for each of the most relevant parameters for EADWs, WACDWs, and EPDWs over various regions. These thresholds are based approximately on the 99% significance level for the sample sizes used for this study. Other future work could involve incorporating these convective indicators that provide the greatest distinction

between developing waves and NDWs in the development of a statistical cyclogenesis/hurricane prediction model.

Acknowledgments. This work was part of the lead author's research for his doctoral degree, and funding for the research was provided through a NASA Earth and Space Science Fellowship (Grant NNX09AO40H). Dr. Walter Petersen and Dr. Daniel Cecil also acknowledge funding from the NASA PMM/TRMM Program. Suggestions from Dr. Ron McTaggart-Cowan and two anonymous reviewers greatly improved earlier versions of this manuscript. The authors would also like to gratefully acknowledge the Goddard Earth Sciences Data and Information Services Center for providing the TMI, PR, and IR brightness temperature data, the NASA EOSDIS Global Hydrology Resource Center DAAC for providing the LIS science data, and the NOAA/OAR/ESRL PSD for providing the NCEP–NCAR reanalysis data.

REFERENCES

Avila, L. A., 1991: Eastern North Pacific hurricane season of 1990. *Mon. Wea. Rev.,* **119,** 2034–2046.

——, and R. J. Pasch, 1992: Atlantic tropical systems of 1991. *Mon. Wea. Rev.,* **120,** 2688–2696.

Awaka, J., T. Iguchi, and K. Okamoto, 1998: Early results on rain type classification by the Tropical Rainfall Measuring Mission (TRMM) precipitation radar. *Proc. Eighth URSI Commission F. Triennial Open Symp.,* Aveiro, Portugal, International Union of Radio Science, 143–146.

——, ——, and ——, 2009: TRMM PR standard algorithm 2A23 and its performance on bright band detection. *J. Meteor. Soc. Japan,* **87A,** 31–52.

Berry, G. J., and C. Thorncroft, 2005: Case study of an intense African easterly wave. *Mon. Wea. Rev.,* **133,** 752–766.

Boccippio, D. J., S. J. Goodman, and S. Heckman, 2000: Regional differences in tropical lightning distributions. *J. Appl. Meteor.,* **39,** 2231–2248.

——, W. J. Koshak, and R. J. Blakeslee, 2002: Performance assessment of the optical transient detector and lightning imaging sensor. Part I: Predicted diurnal variability. *J. Atmos. Oceanic Technol.,* **19,** 1318–1332.

Burpee, R. W., 1972: The origin and structure of easterly waves in the lower troposphere of North Africa. *J. Atmos. Sci.,* **29,** 77–89.

Carlson, T. N., 1969: Synoptic histories of three African disturbances that developed into Atlantic hurricanes. *Mon. Wea. Rev.,* **97,** 256–276.

Cecil, D. J., and E. J. Zipser, 1999: Relationships between tropical cyclone intensity and satellite-based indicators of inner core convection: 85-GHz ice-scattering signature and lightning. *Mon. Wea. Rev.,* **127,** 103–123.

——, and ——, 2002: Reflectivity, ice scattering, and lightning characteristics of hurricane eyewalls and rainbands. Part II: Intercomparison of observations. *Mon. Wea. Rev.,* **130,** 785–801.

——, ——, and S. W. Nesbitt, 2002: Reflectivity, ice scattering, and lightning characteristics of hurricane eyewalls and rainbands. Part I: Quantitative description. *Mon. Wea. Rev.,* **130,** 769–784.

Christian, H. J., 1999: Optical detection of lightning from space. *Proc. 11th Int. Conf. on Atmospheric Electricity,* Guntersville, AL, NASA Conf. Publ. NASA/CP-1999-209261, 715–718. [Available online at http://ntrs.nasa.gov/archive/nasa/casi.ntrs.nasa.gov/19990108601_1999074615.pdf.]

——, R. J. Blakeslee, and S. L. Goodman, 1992: Lightning Imaging Sensor (LIS) for the Earth Observing System. NASA Tech. Memo. NASA TM-4350, 36 pp.

——, and Coauthors, 2003: Global frequency and distribution of lightning as observed from space by the optical transient detector. *J. Geophys. Res.,* **108,** 4005, doi:10.1029/2002JD002347.

Chronis, T. G., E. R. Williams, E. N. Anagnostou, and W. A. Petersen, 2007: African lightning: Indicator of tropical Atlantic cyclone formation. *Eos, Trans. Amer. Geophys. Union,* **88,** 397–398.

Deierling, W., and W. A. Petersen, 2008: Total lightning activity as an indicator of updraft characteristics. *J. Geophys. Res.,* **113,** D16210, doi:10.1029/2007JD009598.

Dunkerton, T. J., M. T. Montgomery, and Z. Wang, 2009: Tropical cyclogenesis in a tropical wave critical layer: Easterly waves. *Atmos. Chem. Phys.,* **9,** 5587–5646.

Farfan, L. M., and J. A. Zehnder, 1997: Orographic influence on the synoptic-scale circulations associated with the genesis of Hurricane Guillermo (1991). *Mon. Wea. Rev.,* **125,** 2683–2698.

Gu, G., R. F. Adler, G. J. Huffman, and S. Curtis, 2004: African easterly waves and their association with precipitation. *J. Geophys. Res.,* **109,** D04101, doi:10.1029/2003JD003967.

Hendricks, E. A., M. T. Montgomery, and C. A. Davis, 2004: The role of ''vortical'' hot towers in the formation of tropical cyclone Diana (1984). *J. Atmos. Sci.,* **61,** 1209–1232.

Hopsch, S. B., C. D. Thorncroft, and K. R. Tyle, 2010: Analysis of African easterly wave structures and their role in influencing tropical cyclogenesis. *Mon. Wea. Rev.,* **138,** 1399–1419.

Houze, R. A., Jr., W.-C. Lee, and M. M. Bell, 2009: Convective contribution to the genesis of Hurricane Ophelia (2005). *Mon. Wea. Rev.,* **137,** 2778–2800.

Iguchi, T., T. Kozu, R. Meneghini, J. Awaka, and K. Okamoto, 2000: Rain-profiling algorithm for the TRMM precipitation radar. *J. Appl. Meteor.,* **39,** 2038–2052.

——, ——, J. Kwiatkowski, R. Meneghini, J. Awaka, and K. Okamoto, 2009: Uncertainties in the rain profiling algorithm for the TRMM precipitation radar. *J. Meteor. Soc. Japan,* **87A,** 1–30.

Kalnay, E., and Coauthors, 1996: The NCEP/NCAR 40-Year Reanalysis Project. *Bull. Amer. Meteor. Soc.,* **77,** 437–471.

Kozu, T., and Coauthors, 2001: Development of precipitation radar onboard the Tropical Rainfall Measuring Mission (TRMM) satellite. *IEEE Trans. Geosci. Remote Sens.,* **39,** 102–116.

Kummerow, C., W. Barnes, T. Kozu, J. Shiue, and J. Simpson, 1998: The tropical rainfall measuring mission (TRMM) sensor package. *J. Atmos. Oceanic Technol.,* **15,** 809–817.

Kurihara, Y., and R. E. Tuleya, 1981: A numerical simulation study on the genesis of a tropical storm. *Mon. Wea. Rev.,* **109,** 1629–1653.

Landsea, C. W., 1993: A climatology of intense (or major) Atlantic hurricanes. *Mon. Wea. Rev.,* **121,** 1703–1713.

Leary, L. A., and E. A. Ritchie, 2009: Lightning flash rates as an indicator of tropical cyclone genesis in the eastern North Pacific. *Mon. Wea. Rev.,* **137,** 3456–3470.

Leppert, K. D., II, and W. A. Petersen, 2010: Electrically active hot towers in African easterly waves prior to tropical cyclogenesis. *Mon. Wea. Rev.,* **138,** 663–687.

——, and D. J. Cecil, 2012: African easterly wave convection and tropical cyclogenesis: A Lagrangian perspective. Preprints, *30th Conf. on Hurricanes and Tropical Meteorology,* Ponte Vedra Beach, FL, Amer. Meteor. Soc., 3C.6. [Available online at https://ams.confex.com/ams/30Hurricane/webprogram/Manuscript/Paper205276/AMS_Trop12_ExtAbst.pdf.]

Liu, Z., D. Ostrenga, G. G. Leptoukh, and A. V. Mehta, 2009: Online visualization and analysis of global half-hourly pixel-resolution infrared dataset. Preprints, *25th Conf. on Interactive Information and Processing Systems (IIPS) for Meteorology, Oceanography, and Hydrology,* Phoenix, AZ, Amer. Meteor. Soc., J3.4. [Available online at https://ams.confex.com/ams/pdfpapers/148189.pdf.]

Meneghini, R., T. Iguchi, T. Kozu, L. Liao, K. Okamoto, J. A. Jones, and J. Kwiatkowski, 2000: Use of the surface reference technique for path attenuation estimates from the TRMM precipitation radar. *J. Appl. Meteor.,* **39,** 2053–2070.

Mohr, K. I., and E. J. Zipser, 1996: Defining mesoscale convective systems by their 85-GHz ice-scattering signatures. *Bull. Amer. Meteor. Soc.,* **77,** 1179–1189.

——, J. S. Famiglietti, and E. J. Zipser, 1999: The contribution to tropical rainfall with respect to convective system type, size, and intensity estimated from the 85-GHz ice- scattering signature. *J. Appl. Meteor.,* **38,** 596–606.

Molinari, J., and D. Vollaro, 2000: Planetary- and synoptic-scale influences on eastern Pacific tropical cyclogenesis. *Mon. Wea. Rev.,* **128,** 3296–3307.

——, D. Knight, M. Dickinson, D. Vollaro, and S. Skubis, 1997: Potential vorticity, easterly waves, and eastern Pacific tropical cyclogenesis. *Mon. Wea. Rev.,* **125,** 2699–2708.

Montgomery, M. T., M. E. Nicholls, T. A. Cram, and A. B. Saunders, 2006: A vortical hot tower route to tropical cyclogenesis. *J. Atmos. Sci.,* **63,** 355–386.

Mozer, J. B., and J. A. Zehnder, 1996: Lee vorticity production by large-scale tropical mountain ranges. Part I: Eastern North Pacific tropical cyclogenesis. *J. Atmos. Sci.,* **53,** 521–538.

National Hurricane Center, cited 2011: NHC archive of hurricane seasons. [Available online at http://www.nhc.noaa.gov/pastall.shtml.]

Nolan, D. S., 2007: What is the trigger for tropical cyclogenesis? *Aust. Meteor. Mag.,* **56,** 241–266.

Norquist, D. C., E. E. Recker, and R. J. Reed, 1977: The energetics of wave disturbances as observed during phase III of GATE. *Mon. Wea. Rev.,* **105,** 334–342.

Panofsky, H. A., and G. W. Brier, 1958: *Some Applications of Statistics to Meteorology.* The Pennsylvania State University, 224 pp.

Price, C., Y. Yair, and M. Asfur, 2007: East African lightning as a precursor of Atlantic hurricane activity. *Geophys. Res. Lett.,* **34,** L09805, doi:10.1029/2006GL028884.

Raymond, D. J., S. L. Sessions, and C. Lopez Carrillo, 2011: Thermodynamics of tropical cyclogenesis in the northwest Pacific. *J. Geophys. Res.,* **116,** D18101, doi:10.1029/2011JD015624.

Reasor, P. D., M. T. Montgomery, and L. F. Bosart, 2005: Mesoscale observations of the genesis of Hurricane Dolly (1996). *J. Atmos. Sci.,* **62,** 3151–3171.

Reed, R. J., D. C. Norquist, and E. E. Recker, 1977: The structure and properties of African wave disturbances as observed during phase III of GATE. *Mon. Wea. Rev.,* **105,** 317–333.

Ritchie, E. A., and G. J. Holland, 1997: Scale interactions during the formation of Typhoon Irving. *Mon. Wea. Rev.,* **125,** 1377–1396.

Rotunno, R., and K. A. Emanuel, 1987: An air–sea interaction theory for tropical cyclones. Part II: Evolutionary study using a non-hydrostatic axisymmetric numerical model. *J. Atmos. Sci.,* **44,** 542–561.

Rutledge, S. A., E. R. Williams, and T. D. Keenan, 1992: The down under Doppler and electricity experiment (DUNDEE): Overview and preliminary results. *Bull. Amer. Meteor. Soc.,* **73,** 3–16.

Saunders, C. P. R., and S. L. Peck, 1998: Laboratory studies of the influence of the rime accretion rate on charge transfer during crystal/graupel collisions. *J. Geophys. Res.,* **103** (D12), 13 949–13 956.

Serra, Y. L., G. N. Kiladis, and M. F. Cronin, 2008: Horizontal and vertical structure of easterly waves in the Pacific ITCZ. *J. Atmos. Sci.,* **65,** 1266–1284.

——, ——, and K. I. Hodges, 2010: Tracking and mean structure of easterly waves over the Intra-Americas Sea. *J. Climate,* **23,** 4823–4840.

Sippel, J. A., J. W. Nielsen-Gammon, and S. E. Allen, 2006: The multiple-vortex nature of tropical cyclogenesis. *Mon. Wea. Rev.,* **134,** 1796–1814.

Smith, E. A., H. J. Cooper, X. Xiang, A. Mugnai, and G. J. Tripoli, 1992: Foundations for statistical-physical precipitation retrieval from passive microwave satellite measurements. Part I: Brightness temperature properties of a time-dependent cloud-radiation model. *J. Appl. Meteor.,* **31,** 506–531.

Spencer, R. W., H. M. Goodman, and R. E. Hood, 1989: Precipitation retrieval over land and ocean with the SSM/I: Identification and characteristics of the scattering signal. *J. Atmos. Oceanic Technol.,* **6,** 254–273.

Takahashi, T., 1978: Riming electrification as a charge generation mechanism in thunderstorms. *J. Atmos. Sci.,* **35,** 1536–1548.

Thorncroft, C. D., N. M. J. Hall, and G. N. Kiladis, 2008: Three-dimensional structure and dynamics of African easterly waves. Part III: Genesis. *J. Atmos. Sci.,* **65,** 3596–3607.

Toracinta, E. R., D. J. Cecil, E. J. Zipser, and S. W. Nesbitt, 2002: Radar, passive microwave, and lightning characteristics of precipitating systems in the tropics. *Mon. Wea. Rev.,* **130,** 802–824.

Williams, E. R., S. A. Rutledge, S. G. Geotis, N. Renno, E. Rasmussen, and T. Rickenbach, 1992: A radar and electrical study of tropical "hot towers." *J. Atmos. Sci.,* **49,** 1386–1395.

Yang, S., W. S. Olson, J.-J. Wang, T. L. Bell, E. A. Smith, and C. D. Kummerow, 2006: Precipitation and latent heating distributions from satellite passive microwave radiometry. Part II: Evaluation of estimates using independent data. *J. Appl. Meteor. Climatol.,* **45,** 721–739.

Zehnder, J. A., 1991: The interaction of planetary-scale tropical easterly waves with topography: A mechanism for the initiation of tropical cyclones. *J. Atmos. Sci.,* **48,** 1217–1230.

——, D. M. Powell, and D. L. Ropp, 1999: The interaction of easterly waves, orography, and the intertropical convergence zone in the genesis of eastern Pacific tropical cyclones. *Mon. Wea. Rev.,* **127,** 1566–1585.

Zipser, E. J., 1994: Deep cumulonimbus cloud systems in the tropics with and without lightning. *Mon. Wea. Rev.,* **122,** 1837–1851.